

p53 and Mitochondrial DNA

Their Role in Mitochondrial Homeostasis and Toxicity of Antiretrovirals

Christopher A. Koczor, Richard C. White,
Peter Zhao, Linjue Zhu, Earl Fields, and
William Lewis

*From the Department of Pathology, Emory University, Atlanta,
Georgia*

The roles and actions of the tumor suppressor protein p53 have been extensively studied with regard to nuclear events, including transcription and DNA damage repair. However, the direct roles of p53 in mitochondrial DNA (mtDNA) replication and function are less well understood. Studies herein used a mitochondrial-targeted p53 (MTS-p53) to determine its effects on both mtDNA abundance and mitochondrial function. MTS-p53 decreased cellular proliferation and mtDNA abundance in HepG2 cells transfected with wild-type (WT) human p53. When MTS-p53 cells were treated with the nucleoside reverse transcriptase inhibitor (NRTI), 2',3'-dideoxycytidine or 2',3'-dideoxyinosine, mtDNA depletion that resembled untransfected controls was observed in both instances. p53-Overexpressing cells showed reduced mitochondrial function by oximetry, including a reduction in maximal respiratory capacity and reserve capacity. A truncated p53 (MTS-p53-290) was generated for localization exclusively to the mitochondria. MTS-p53-290 cells proliferated at control levels but displayed decreased mtDNA abundance and mitochondrial function with NRTI treatment. The MTS-p53-290 cells demonstrated that only the nuclear fraction of p53 controlled cellular proliferation, which was supported by the MTS-p53 results. Data herein indicate that overexpression of p53 in the mitochondria reduces mtDNA abundance and increases the sensitivity of mammalian cells to NRTI exposure by reducing mitochondrial function. (*Am J Pathol* 2012, 180:2276–2283; <http://dx.doi.org/10.1016/j.ajpath.2012.01.045>)

Tumor suppressor protein p53 is characterized as a guardian of the genome, with various functions as a tran-

scription factor, DNA damage repair modulator, and signaling protein.^{1–3} In addition to those nuclear functions, p53 plays an important role in mitochondrial-mediated cellular responses, including the binding of proteins localized to the outer mitochondrial membrane that initiates apoptosis.^{4–7} Evidence has suggested that p53 is present and functions in the mitochondrial matrix.^{8–11}

Determination of the mitochondrial matrix localization for native p53 has not been fully established. Mass spectrometry analysis of mitochondrial nucleoids failed to detect the presence of p53,^{12,13} whereas others^{8–11} show that p53 binds to mitochondrial DNA (mtDNA) and aids in mtDNA repair. The p53 within the cell is helpful in maintaining normal mitochondrial function because p53 in the mitochondria enhances base excision repair of mtDNA damage,^{9–11} and a loss of cellular p53 reduces mitochondrial function.^{14,15} Such enhancement of mtDNA repair would have a positive impact on mitochondrial function and biogenesis.

Experiments herein were designed to determine the role of p53 in the mitochondria of mammalian cells. To accomplish this, a plasmid construct containing a mitochondrial-targeting sequence (MTS) ligated to the N-terminus of the p53 protein (MTS-p53) was used to target mitochondrial translocation of p53. Because of the strong intrinsic nuclear localization of MTS-p53 as the result of the sequence located in the 291 to 393 amino acid region of p53, a second truncated construct of p53 (MTS-p53-290) was generated to reduce nuclear localization of the protein. The p53 translocated to the mitochondria in both cases, with nuclear localization of p53 only seen in the MTS-p53 construct. The mitochondrial-localized p53 overexpression resulted in depleted mtDNA abundance

Supported by a grant from the National Institute on Drug Abuse/NIH/U.S. Department of Health and Human Services (DA030996 to W.L.) and a grant from the National Heart, Lung, and Blood Institute/NIH/U.S. Department of Health and Human Services (HL079867 to W.L.).

Accepted for publication January 30, 2012.

Address reprint requests to Christopher A. Koczor, Ph.D., Department of Pathology, Emory University, 101 Woodruff Cir, Woodruff Memorial Research Building 7205, Atlanta, GA 30322. E-mail: ckoczor@emory.edu.

and a reduction in oxidative function in the face of treatment with pharmacological doses of nucleoside reverse transcriptase inhibitors (NRTIs), 2',3'-dideoxycytidine (ddC) and 2',3'-dideoxyinosine (ddI). Increased mitochondrial-targeted p53 negatively regulates mitochondrial function and mtDNA abundance, and our findings suggest that one new role of p53 in the mitochondria is the regulation of mitochondrial biogenesis.

Materials and Methods

Plasmid Construction and Transfection

A CMV vector plasmid containing WT human p53 (Clontech, Mountain View, CA) was restricted with BamHI (Fermentas, Glen Burnie, MD) and Eco0109I (New England Biolabs, Ipswich, MA) to release the p53 insert and truncate the stop codon. High-fidelity PCR using Pfx (Invitrogen, Grand Island, NY) was used to engineer an N-terminal MTS and a C-terminal hemagglutinin (HA) tag onto the p53 protein. The N-terminal primer was developed to add the MTS of ornithine transcarbamylase to the N-terminus of the p53 protein (sequence, 5'-GAGAGAGTCGACGCCACCATGCTGTTAATCTGAGGATCCTGTTAAACAATGCAGCTTTTAGAAATGGTCACAACCTCATGGTTCGAAATTTAAGCTTATGGAGGAGCCGCAG-3'). The C-terminal primer was developed to add the HA tag to the C-terminus of the p53 protein to enable discrimination of the additional p53 from endogenous p53 (sequence, 5'-TCTCTCGTCTGACTCAAGCGTAGTCTGGGACGTCGATGGGTAGTCTGAGTCAGGCCCTTCTGTCTTGAACATGAGTTT-3'). The resulting MTS-p53 construct was gel purified and ligated back into the CMV vector plasmid using blunt-end ligation. The resulting ligation product was grown in NEB5 α cells (New England Biolabs), which were clonally selected, and the purified plasmid was sequenced to ensure fidelity.

The MTS-p53-290 construct was generated using the Stratagene QuikChange site-directed mutagenesis kit (Agilent, Santa Clara, CA). BsiWI restriction enzyme sites were introduced into the MTS-p53 construct at sites 290 to 291 and 391 to 392 using specially designed primers, following the recommendations of the manufacturer. The resulting plasmid was restricted with BsiWI (Fermentas) to release the 291 to 391 region of p53 and ligated back together. The resulting ligation product (termed MTS-p53-290) was grown in NEB5 α cells, which were clonally selected, and the purified plasmid was sequenced to ensure fidelity.

HepG2 cells were grown in Eagle's minimal essential medium (American Type Culture Collection, Manassas, VA) with 10% fetal bovine serum (American Type Culture Collection) and penicillin-streptomycin (Invitrogen) at 37°C and 5% CO₂. Cells were transfected with either the MTS-p53 or the MTS-p53-290 plasmid using the Fugene 6 transfection reagent (Roche, Indianapolis, IN) in a 3:1 ratio. Vector cells received only the CMV plasmid without the MTS-p53. Cells were transfected for 24 hours, then trypsinized and reseeded in Eagle's minimal essential medium containing 600 μ g/mL G418 (Lonza, Hopkinton,

MA) to select for positive clones. After 14 days of G418 selection, colonies were selected using cloning cylinders and were determined positive for the insert using primers against the full-length region surrounding the MTS-p53 or MTS-p53-290 insert (forward, 5'-TGGAAAAACGCCAGCAACGCG-3'; reverse, 5'-AAGGGATTTGCCGATTTCCGAA-3'). Positive colonies were verified for protein presence and localization by standard SDS-PAGE and Western blot protocols using an HA antibody (Sigma-Aldrich, St. Louis, MO) for the MTS-p53 protein, human p53 antibody (Novus Biologicals, Littleton, CO) for the MTS-p53-290 protein, succinate dehydrogenase subunit B (Novus Biologicals) as a mitochondrial marker, and lamin A (Sigma-Aldrich) as a nuclear marker. Subcellular fractionation was achieved through differential centrifugation after saponin treatment to permeabilize the cell membrane.

Cell Viability

The following reagents were obtained through the AIDS Research and Reference Reagent Program, Division of AIDS, National Institute of Allergy and Infectious Diseases, NIH: ddC (zalcitabine) and ddI (didanosine). Cells were plated at 1×10^5 cells per well in a six-well dish. Cells were allowed to proliferate for 24 hours in the absence of ddC or ddI. After the initial 24 hours, ddC (1.0 or 10.0 μ mol/L) or ddI (10.0 or 100.0 μ mol/L) was added to the media, and the cells were collected and counted after 72 hours of additional growth. Cells were trypsinized and counted using the trypan blue exclusion assay and a hemocytometer.

mtDNA Abundance

Cells were plated at 1×10^5 cells per well in a six-well dish. Cells were allowed to proliferate for 24 hours in the absence of ddC or ddI. After the initial 24 hours, ddC (0.1, 0.3, 1.0, 3.0, or 10.0 μ mol/L) or ddI (10, 30, or 100 μ mol/L) was added to the media, and the cells were lysed after 24, 48, or 72 hours of growth using one times Tris-EDTA with 30 μ g/mL of proteinase K (Invitrogen) and 0.5% SDS. Samples were allowed to lyse for 24 hours at 37°C. After lysis, the DNA was extracted from each sample using the MagNA Pure LC (Roche). The resulting DNA samples were quantitated and analyzed for mtDNA abundance using the Lightcycler 480 (Roche). Nuclear DNA was amplified using the single-copy *POLG2* nuclear gene (forward, 5'-GAGCTGTTGACGGAAAGGAG-3'; reverse, 5'-CAGAAGAGAATCCCGGCTAA-3'), and mtDNA was amplified using the *COXI* mitochondrial gene (forward, 5'-TTCGCCGACCGTTGACTATT-3'; reverse, 5'-AAGATTATTACAAATGCATGGGC-3').

Oximetric Analysis

Oximetry and analysis were performed using an XF24 extracellular flux analyzer (Seahorse Bioscience, Billerica, MA) using methods described by the manufacturer. HepG2 vector, MTS-p53 clone 2 cells, and MTS-p53-290 cells were seeded at 3×10^4 cells per well into

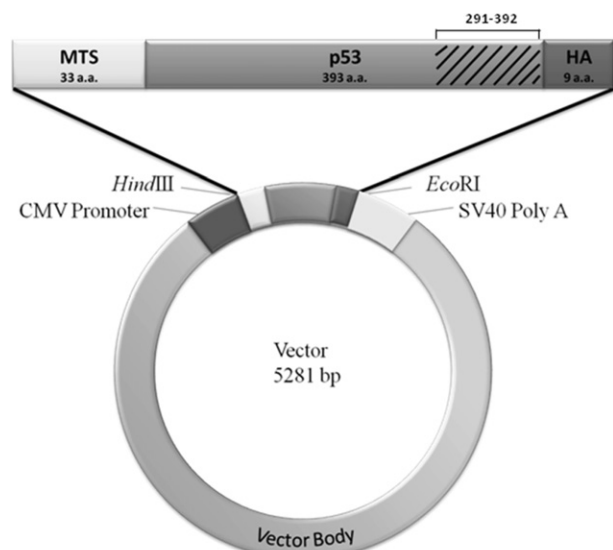


Figure 1. MTS-p53 and MTS-p53-290 construct map. The MTS of ornithine transcarbamylase was added to the N-terminal side of human WT p53, and an HA tag was added to the C-terminal side of p53 to discriminate between the additional p53 from the endogenous p53. The shaded area shows the location of the truncated 291 to 393 region of the MTS-p53-290 protein. The constructs were placed under a CMV promoter and selected by geneticin in HepG2 cells. a.a., amino acid.

an XF24 V7 plate (Seahorse Bioscience). Cells were allowed to grow for 24 hours in normal growth media. After the initial 24 hours, cells were treated with ddC (0.1, 1.0, or 10.0 $\mu\text{mol/L}$) or ddl (1.0, 10.0, or 100.0 $\mu\text{mol/L}$) for 24 or 72 hours. After 24 or 72 hours, media were aspirated from the XF24 wells, unbuffered Dulbecco's modified Eagle's medium (Seahorse Bioscience) was supplemented with 4 mmol/L glucose (Sigma-Aldrich), and 1 mmol/L sodium pyruvate (Sigma-Aldrich) was added to each well. Cells were allowed to equilibrate in the new media for 30 minutes before analysis by the XF24 system. Cells were sequentially exposed to oligomycin (1 $\mu\text{g/mL}$; Sigma-Aldrich), fluoro-carbonyl cyanide phenylhydrazine (1.0 $\mu\text{mol/L}$; Sigma-Aldrich), and rotenone (2.0 $\mu\text{mol/L}$; Sigma-Aldrich) to determine cellular and mitochondrial oxygen consumption rates (OCRs). Data are expressed as a percentage of the OCRs of the untreated controls. Results from these experiments were used to determine basal respiration, proton leakage (defined as the difference between basal respiration OCR and nonmitochondrial OCR after rotenone treatment), maximal respiration (defined as the maximum OCR after fluoro-carbonyl cyanide phenylhydrazine uncoupling), and reserve capacity (defined as the difference between the maximum respiration OCR and the basal respiration OCR).

Statistical Analysis

All experiments were performed with $n \geq 3$, with significance determined using a one-way analysis of variance or a two-tailed Student's *t*-test, where appropriate, with $P < 0.05$ (GraphPad Prism, La Jolla, CA). A Tukey post hoc test was performed for each data set, along with a Grubbs test to determine outliers.

Results

In the plasmid construct, the MTS of ornithine transcarbamylase was ligated to the N-terminus of the WT p53 protein (Figure 1), as previously used to translocate cytosolic proteins into the mitochondria.¹⁶ The addition of a C-terminal HA tag helped verify that p53 translocated to the mitochondria and was separate from any endogenous p53. Two clones expressed the MTS-p53-containing construct (Figure 2A). By using an HA antibody, Western blot analyses were performed on fractionated extracts. The MTS-p53 protein localized to the mitochondrial-enriched fraction and the nuclear fraction (Figure 2B). Both MTS-p53 clones 2 and 3 were used to reduce misinterpretation of clonal expansion effects.

The cell viability and proliferation rates of the vector and MTS-p53 cells were determined using the trypan blue exclusion assay. The empty vector and both MTS-p53 clones were seeded at the same initial cell density and allowed to proliferate for 72 hours. After 72 hours, both MTS-p53-overexpressing clones showed a significant decrease (approximately 50%) in counted cells compared with the vector clones (Figure 3A). There was no change in cell viability (Figure 3B). Rates of doubling revealed that MTS-p53 clones doubled at a slower rate (clone 2, 20.7 hours; clone 3, 17.9 hours) compared with empty vector controls (15.4 hours). This observed decrease correlated with the amount of p53 expressed in the cells based on immunoblot analysis.

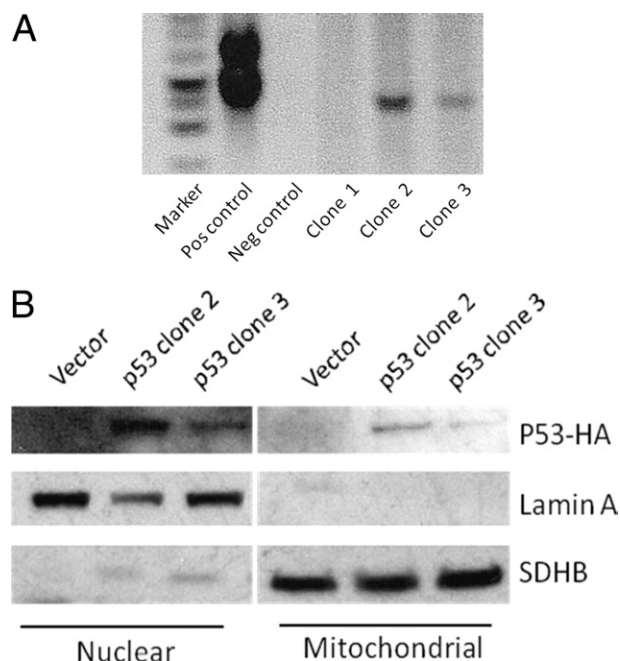


Figure 2. MTS-p53-overexpressing clones. The p53 clones were characterized by PCR genotyping and Western blot analysis. **A:** PCR genotyping demonstrates that clones 2 and 3 were positive (Pos) for the MTS-p53 insert. Neg, negative. **B:** SDS-PAGE and Western blot analysis show that p53 clones 2 and 3 expressed the MTS-p53 in both the nuclear and mitochondrial fraction. An HA antibody was used to determine the amount of p53 produced from the MTS-p53 construct, with succinate dehydrogenase subunit B (SDHB; a mitochondrial marker) and lamin A (a nuclear marker) used as protein fraction markers.

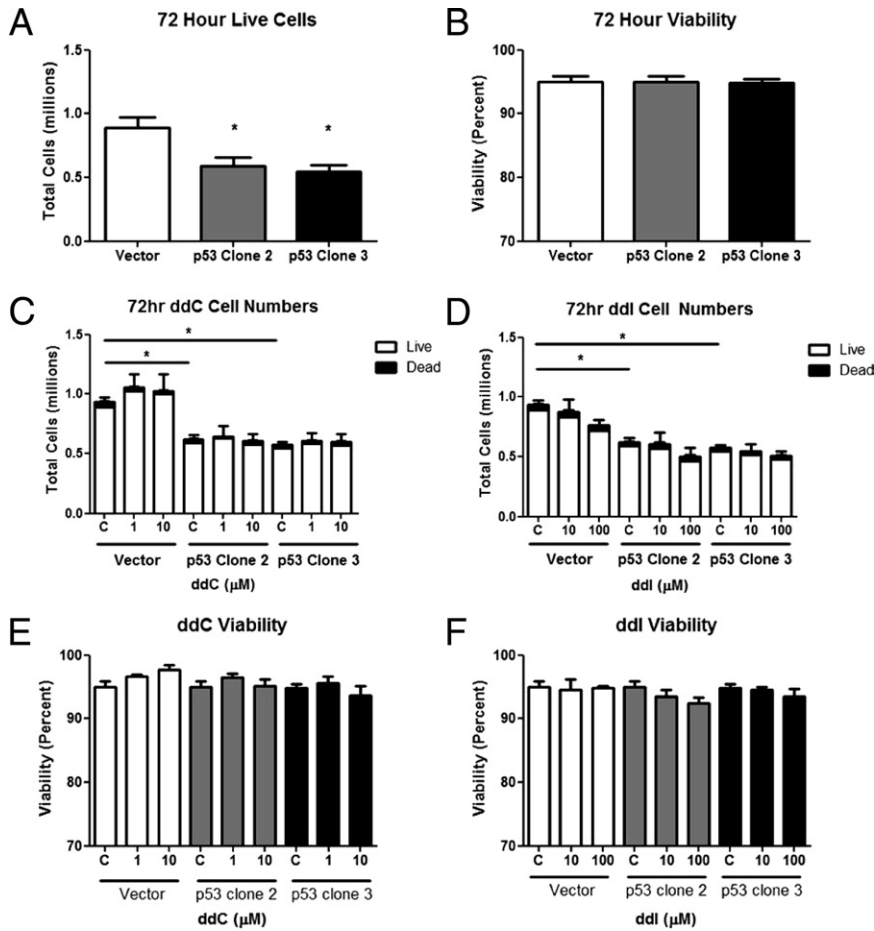


Figure 3. Cellular proliferation and viability of MTS-p53 cells. Vector and MTS-p53 clones were allowed to proliferate for 72 hours in either the presence or the absence of ddC or ddl. Untreated MTS-p53 clones showed a decrease in cellular proliferation compared with the vector-only clone (A), whereas there was no increase in cell death (B). The treatment of clones with ddC over a broad range did not elicit a change in either cell proliferation (C) or cell death (E) compared with their untreated controls (C). The treatment of clones with ddl over a broad range also did not elicit a change in cell proliferation (D) or cell death (F) compared with the untreated controls. **P* < 0.05.

We determined the sensitivity of the clones to mtDNA depletion by adding NRTIs, ddC and ddl. Both of the compounds have been used to treat patients with human immunodeficiency virus 1 or are currently in use. These NRTIs were toxic and caused severe mtDNA depletion.¹⁷ Doses used resemble those used in previous studies,¹⁸ and there was no appreciable decrease in cellular proliferation at 72 hours after ddC or ddl, compared with untreated controls (Figure 3, C and D). Neither ddC nor ddl exposure reduced the viability of the cells (Figure 3, E and F, respectively).

We focused on a possible contribution of the mitochondrial-targeted p53 to alterations in mtDNA abundance. We analyzed the mtDNA abundance of all three clones using real-time PCR. Results showed a modest, statistically significant, 25% decrease in mtDNA abundance in both of the MTS-p53 cell lines when compared with the controls (Figure 4A). These results demonstrate that overexpression of p53 negatively affects the mtDNA abundance in HepG2 cells. Treatment of the cells with ddC decreased mtDNA abundance in both a dose- and time-dependent manner (Figure 4, B–F). Depletion of mtDNA became apparent after 24 hours of exposure at the lowest doses of ddC, and mtDNA depletion worsened with duration of exposure. A dose-dependent decrease in mtDNA abundance resulted from ddl treatment after 72 hours (Figure 4, G and H). Overexpression of MTS-p53

did not affect NRTI-induced mtDNA depletion, based on either the concentration of NRTI treatment or the duration of exposure. Overall, these data suggest that overexpression of p53 does not protect cells from ddC- or ddl-induced mtDNA depletion at the doses used. Moreover, NRTI-induced mtDNA depletion does not directly affect cellular viability or cell proliferation.

To determine the effects of ddC and ddl on mitochondrial electron transport, we used an XF24 analyzer (Seahorse Bioscience) to measure cellular OCRs. The cells were plated and exposed to ddC and ddl in a similar manner to the mtDNA abundance experiments, although only the vector and MTS-p53 clone 2 were used for these experiments that determined cellular OCRs. After 24 or 72 hours of 10 μmol/L ddC, a significant decrease in basal respiration in the MTS-p53 clone was found (Figure 5A). There was no change in proton leakage, suggesting the absence of apoptosis through the intrinsic pathway (Figure 5B). Data suggest that mitochondrial permeabilization is not increased and that MTS-p53 does not promote apoptosis of the cells after ddC exposure. In addition, there was a decrease in the maximal respiration of the MTS-p53 clone and in the reserve capacity of the p53 clone after ddC (Figure 5, C and D, respectively). These results show that p53 sensitizes the cells to ddC exposure in an mtDNA-independent mechanism and that the

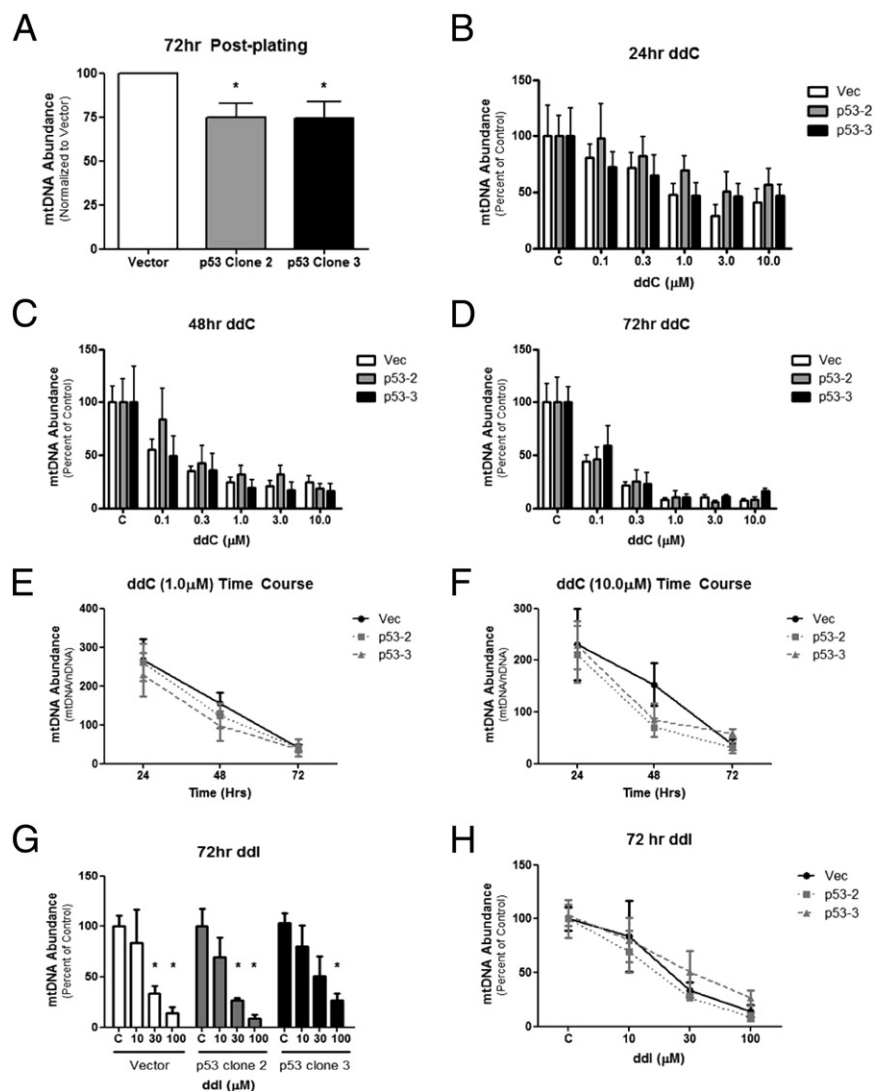


Figure 4. The mtDNA abundance in MTS-p53 cells. The vector (Vec) and MTS-p53 clones were treated with either ddC or ddi for 24, 48, or 72 hours and then lysed to analyze mtDNA abundance by real-time PCR. **A:** Untreated MTS-p53 clones showed a decrease in mtDNA abundance compared with the vector-only controls (C). Exposure to ddC elicited a dose-dependent reduction at 24 hours (**B**), 48 hours (**C**), and 72 hours (**D**) in mtDNA abundance in MTS-p53 and empty vector cells. There was no difference in the rate of mtDNA depletion after 1.0 $\mu\text{mol/L}$ (**E**) or 10.0 $\mu\text{mol/L}$ (**F**) of ddC exposure in MTS-p53 or vector cells. Similar dose-dependent results could be seen after ddi exposure (**G**), with no differences between vector and MTS-p53 cells (**H**). * $P < 0.05$.

ability to produce energy is reduced in MTS-p53 cells after ddC treatment.

Similar results were seen with the ddi experiments, although ddi had a more appreciable effect on mitochondrial OCR on the vector-only cells, compared with ddC. There was no difference in basal respiration or proton leakage after ddi (**Figure 5, E and F**). However, ddi reduced maximal respiration and reserve capacity in the MTS-p53 clones (**Figure 5, G and H**). These data demonstrate that overexpressing p53 sensitizes the cells to NRTI exposure by reducing maximal respiration and reserve capacity.

To control for the nuclear localization of the MTS-p53 protein, a construct was generated to remove its nuclear localization sequence. The nuclear localization sequence is located in the 291 to 393 amino acid region of p53, and we generated the second construct (termed MTS-p53-290) to remove this region while still expressing the enzymatic and DNA-binding domains located in the 1 to 290 amino acid region.^{19,20} This construct retained the original MTS from ornithine transcarbamylase to promote mitochondrial localization. Immunoblots show that the

MTS-p53-290 protein product was exclusively localized to the mitochondrial compartment (**Figure 6**). Cell proliferation studies revealed that the MTS-p53-290-transfected cells proliferated at the same rate as the vector-only cells, demonstrating that overexpression of p53 in the nuclear compartment was responsible for the increased doubling times seen in the MTS-p53 clones (**Figure 7A**). There was no change in cell viability in untreated cells (**Figure 7B**). Furthermore, there were no changes seen in proliferation or viability after ddC (**Figure 7, C and E, respectively**) or ddi (**Figure 7, D and F, respectively**) treatment, demonstrating that MTS-p53-290 does not affect proliferation or viability over the doses or times studied.

Changes in mtDNA abundance were analyzed after ddC and ddi exposure in the MTS-p53-290 cells. Similar to the MTS-p53 cells, MTS-p53-290 cells showed a reduction in mtDNA abundance in untreated cells when compared with vector-only cells (**Figure 8A**). There was a 40% reduction in mtDNA abundance in MTS-p53-290 cells when compared with controls. When treated with ddC or ddi, data show a dose-dependent decrease in

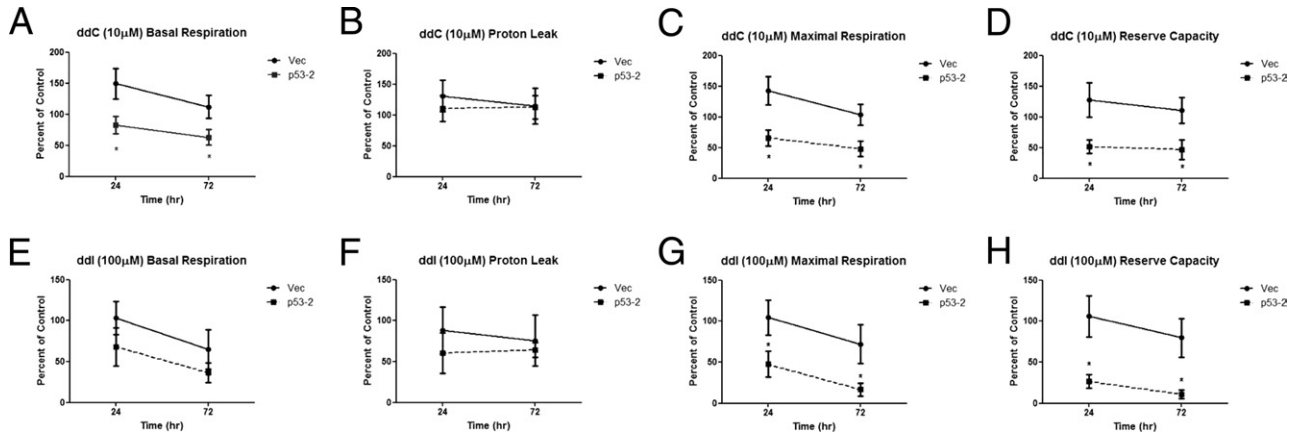


Figure 5. The OCRs of MTS-p53 cells. Vector (Vec) and p53 clone 2 mitochondrial function was determined using an XF24 flux analyzer. Cells were treated with ddC (A–D) or ddl (E–H) for 24 or 72 hours and then analyzed for OCR. MTS-p53 cells showed a marked decrease in basal respiration after ddC treatment (A), whereas ddl elicited a small, but not statistically significant, decrease in basal respiration (E). There was no change in proton leakage after ddC (B) or ddl (F) exposure, suggesting no increase in mitochondrial permeabilization, often seen during apoptosis. Both ddC and ddl significantly reduced the maximal respiration (C and G, respectively) and reserve capacity (D and H, respectively) when normalized to untreated cells. **P* < 0.05.

mtDNA abundance with increasing doses of ddC and ddl, and this effect was independent of p53 abundance in the mitochondria (Figure 8, B and C, respectively). There was no statistical difference between MTS-p53-290 mtDNA abundance after ddC or ddl treatment when compared with similar doses in control cells. These studies show that overexpression of p53 in the mitochondria does not protect cells from ddC- or ddl-induced mtDNA depletion at the doses used, similar to results seen in the MTS-p53 cells.

Finally, oxygen consumption measurements were performed on the MTS-p53-290 cells. Experiments showed that MTS-p53-290 cells were sensitized to ddC and ddl at the highest doses used. Overexpression of p53 in the mitochondria reduced basal respiration, maximal respiration, and reserve capacity after ddC and ddl exposure, whereas vector cells remained unchanged (Figure 9). There was no change in proton leakage after ddC or ddl treatment. These experiments demonstrate that p53 in the mitochondria sensitizes the cells to NRTI exposure,

independent of changes in mtDNA abundance, by reducing electron transport function.

Discussion

This work demonstrates that overexpression of p53 negatively affects the normal mitochondrial homeostasis in

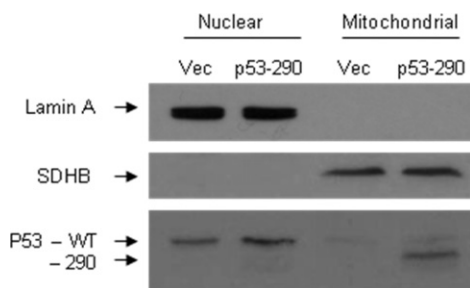


Figure 6. MTS-p53-290 subcellular localization. The 291 to 393 amino acid region of WT human p53 was truncated as described in *Materials and Methods*. This construct contains the MTS from ornithine transcarbamylase. The reduced size of the MTS-p53-290 protein produced a unique band that was easily differentiated from WT p53. Subcellular fractionation revealed that the MTS-p53-290 protein localized exclusively to the mitochondrial fraction, with no visible MTS-p53-290 protein in the nuclear fraction. A human p53 antibody was used to determine the amount of p53 produced from the MTS-p53-290 construct, with succinate dehydrogenase subunit B (SDHB; a mitochondrial marker) and lamin A (a nuclear marker) used as protein fraction markers.

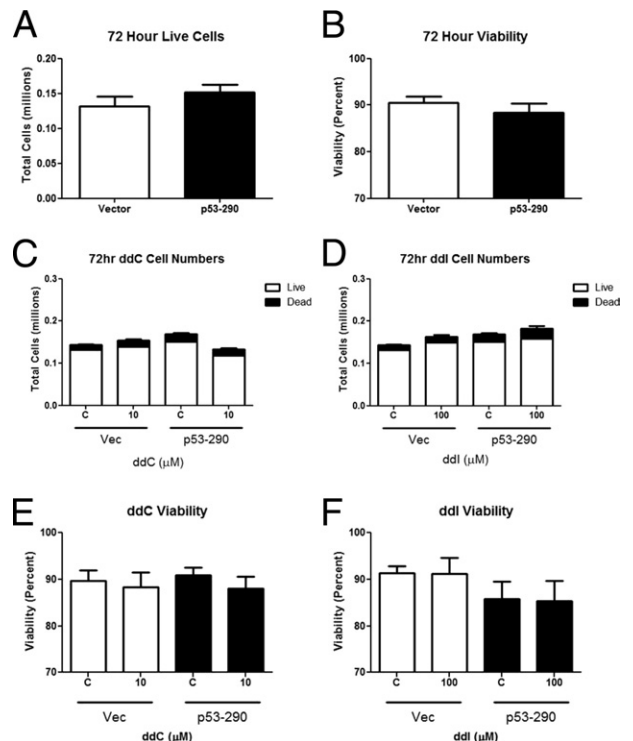


Figure 7. Cellular proliferation and viability of MTS-p53-290 cells. Vector (Vec) and MTS-p53-290 clones were allowed to proliferate for 72 hours in either the presence or the absence of ddC or ddl. Untreated MTS-p53-290 cells showed no change in cellular proliferation (A) or viability (B) compared with the vector-only cells. Treatment of cells with ddC did not elicit a change in either cell proliferation (C) or cell death (E) compared with their untreated controls (C). Treatment of cells with ddl also did not elicit a change in cell proliferation (D) or cell death (F) compared with the untreated controls.

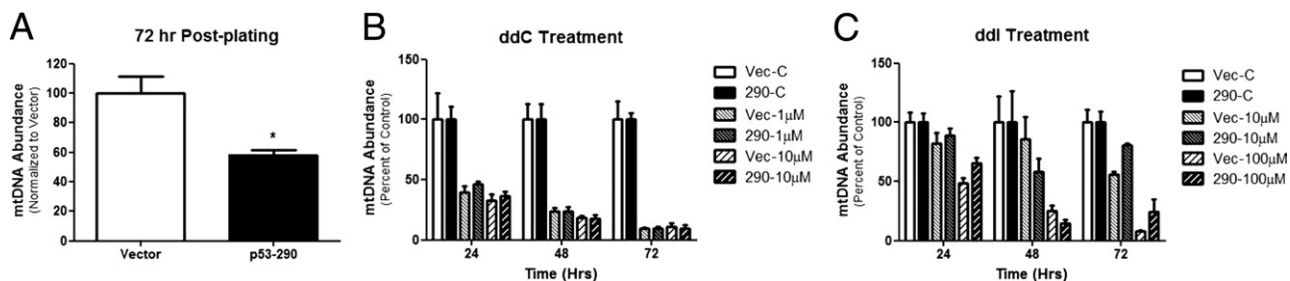


Figure 8. The mtDNA abundance in MTS-p53-290 cells. Vector and MTS-p53-290 clones were treated with either ddC or ddiI for 24, 48, or 72 hours and then lysed to analyze mtDNA abundance. **A:** Untreated MTS-p53-290 cells showed a 40% decrease in mtDNA abundance compared with the vector-only controls (C). Exposure to ddC elicited a reduction in mtDNA abundance in MTS-p53-290 and empty vector cells (**B**). There was no difference in the rate of mtDNA depletion after 1.0 or 10.0 $\mu\text{mol/L}$ of ddC exposure in the p53 of vector cells. Similar results could be seen after ddiI exposure (**C**), with no statistical differences between vector and the MTS-p53-290 cells at any of the times or doses used. * $P < 0.05$.

the cells, decreases mtDNA abundance, and enhances sensitivity to NRTIs that deplete mtDNA. p53 has been studied extensively in the nucleus and cytosol, whereas the mitochondrial role of p53 has focused on a membrane-bound fraction and its role in promoting apoptosis.⁴⁻⁷ The constructs used herein in experiments were designed to minimize overexpression of p53 in the nu-

cleus of the cells and maximize mitochondrial localization. We found that the MTS used was not strong enough to completely overcome the nuclear localization inherent to p53.^{19,20} This resulted in overexpression of p53 in both the nuclear and mitochondrial fractions, with each fraction contributing to the observed results in the MTS-p53 studies. Truncation of the 291 to 391 portion of p53, along with attachment of an MTS, enabled selective localization of the MTS-p53-290 protein to the mitochondria and further discrimination of the results seen in the MTS-p53 studies. The MTS-p53-290 studies allowed us to discriminate the results of the MTS-p53 studies into those relating to nuclear overexpression of p53 and mitochondrial overexpression of p53.

Results showed that overexpression of MTS-p53 decreased cell proliferation (Figure 3A). This effect can be attributed to the nuclear fraction of the MTS-p53 protein because a decrease in cellular proliferation was not seen in the MTS-p53-290 cells (Figure 7A). We also found no change in cellular proliferation or viability in either p53 cell after ddC or ddiI treatment. Because both of these compounds are mitochondrial toxic and did not change proliferation or viability, these data validate that the decrease in cellular proliferation was a contribution of the nuclear p53 and not a result of mitochondrial-localized p53.

Overexpression of the p53 constructs used in these experiments decreased mtDNA abundance (Figures 4A and 8A). The manner in which p53 is able to reduce mtDNA abundance is unknown. Previous work¹⁴ has shown that decreased levels of p53 lead to a decrease in mtDNA abundance, whereas in our research, higher levels of p53 can lead to a decrease in mtDNA abundance. These results could be explained by the difference in functions and subcellular localization of the p53 protein. Because of p53's transcription factor activity in the nucleus, a loss of p53 in the nucleus would reduce mitochondrial proteins required for mtDNA maintenance. In our studies, because there is no change in nuclear p53 status in the MTS-p53-290 clones, there would be no changes in the nuclear transcriptional activity of the endogenous p53. The MTS-p53-290 cells enable for the elucidation of the mitochondrial p53 function, independent of previous studies of nuclear p53 functions. These findings would implicate an inherent p53 activity that

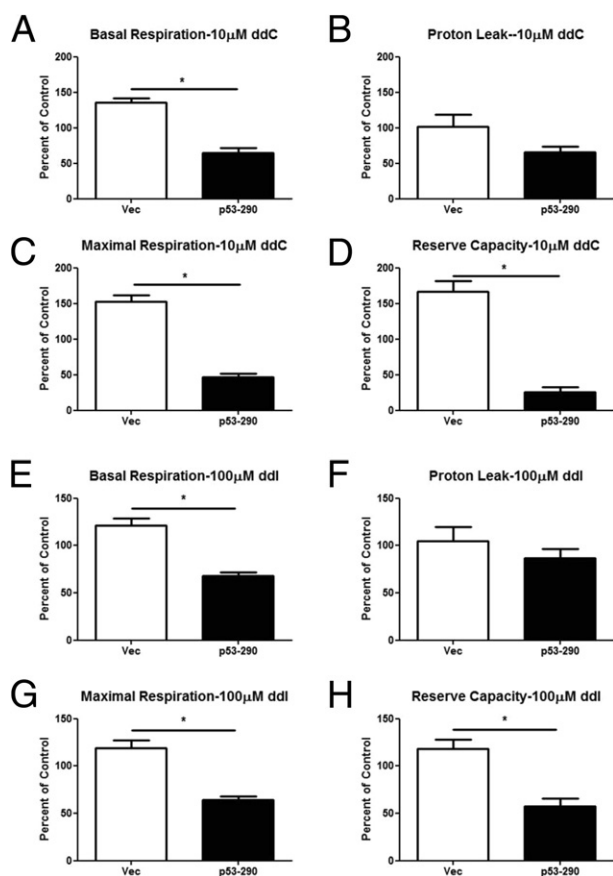


Figure 9. The OCRs of MTS-p53-290 cells. Vector (Vec) and MTS-p53-290 mitochondrial function was determined using an XF24 flux analyzer. Cells were treated with ddC (**A-D**) or ddiI (**E-H**) for 72 hours and then analyzed for OCRs. MTS-p53-290 cells displayed decreased basal respiration after ddC (**A**) and ddiI (**E**) treatment. There was no change in proton leakage after ddC (**B**) or ddiI (**F**) exposure. Both ddC and ddiI significantly reduced the maximal respiration (**C** and **G**, respectively) and reserve capacity (**D** and **H**, respectively) when normalized to untreated cells. * $P < 0.05$.

would enable a loss of mtDNA in the MTS-p53 and MTS-p53-290 cells as a result of mitochondrial expression.

There is the possible role of p53's exonuclease function negatively affecting mtDNA abundance. The p53 has had an intrinsic 3' to 5' exonuclease function that can be used to aid in base excision repair.^{9,21} This presents at least three possibilities. In the first case, p53 may be aiding the repair of endogenous damage present in mtDNA. In this case, more complete copies of mtDNA would enable quicker transcription of electron transport proteins to meet energy demands. This would require a smaller pool of low-damage mtDNA that can be used more efficiently than higher-damage mtDNA but would make that smaller pool of mtDNA more susceptible to mtDNA genotoxic stress, as seen after ddC and ddl exposure. The second possibility is that p53's exonuclease activity is promoting digestion of more damaged copies of mtDNA. Previous work²² has shown that overexpression of robust exonuclease function of exonuclease III in the mitochondria can lead to mtDNA depletion and initiate cell death. However, we do not see any changes in cell viability and we do not know the levels of damage present in these cells. The final possibility is an unknown mitochondrial function of p53 for negatively regulating mtDNA abundance.

Oximetry demonstrated that p53 sensitized the cells to ddC and ddl treatment. These changes in OCR are attributed to the mitochondrial fraction of p53. ddC and ddl are known inhibitors of mtDNA replication, the primary cause of their toxicity in humans.¹⁷ The diminished OCR in the p53 clone after ddC and ddl suggests a threshold effect for mtDNA depletion. The MTS-p53 clones exhibited a 25% decrease in mtDNA compared with the vector clones, whereas the MTS-p53-290 cells exhibited a 40% decrease in mtDNA compared with the vector clones. Treatment with ddC or ddl caused a significant depletion of mtDNA at each dose. Once mtDNA depletion reaches a functional threshold, mitochondrial electron transport defects may result from depleted mtRNA and lower mitochondrial protein abundance.

Our results show that mitochondrial overexpression of p53 leads to decreased mitochondrial function and diminished mtDNA abundance. The mechanism of p53's control of mitochondrial electron transport and cellular energetics is important for understanding the changes in mitochondrial function after cellular stresses, such as oxidative stress or antiretroviral therapies. Delineating the function of each localized fraction of p53 will help determine p53's contribution to mtDNA abundance and oxidative phosphorylation.

References

- Carson DA, Lois A: Cancer progression and p53. *Lancet* 1995, 346:1009–1011
- Efeyan A, Serrano M: p53: Guardian of the genome and policeman of the oncogenes. *Cell Cycle* 2007, 6:1006–1010
- Tokino T, Nakamura Y: The role of p53-target genes in human cancer. *Crit Rev Oncol Hematol* 2000, 33:1–6
- Lozano G: Mouse models of p53 functions. *Cold Spring Harb Perspect Biol* 2010, 2:a001115
- Vaseva AV, Moll UM: The mitochondrial p53 pathway. *Biochim Biophys Acta* 2009, 1787:414–420
- Marchenko ND, Zaika A, Moll UM: Death signal-induced localization of p53 protein to mitochondria: a potential role in apoptotic signaling. *J Biol Chem* 2000, 275:16202–16212
- Mihara M, Erster S, Zaika A, Petrenko O, Chittenden T, Pancoska P, Moll UM: p53 Has a direct apoptogenic role at the mitochondria. *Mol Cell* 2003, 11:577–590
- Canugovi C, Maynard S, Bayne AC, Sykora P, Tian J, de Souza-Pinto NC, Croteau DL, Bohr VA: The mitochondrial transcription factor A functions in mitochondrial base excision repair. *DNA Repair (Amst)* 2010, 9:1080–1089
- Bakhanashvili M, Grinberg S, Bonda E, Simon AJ, Moshitch-Moshkovitz S, Rahav G: p53 In mitochondria enhances the accuracy of DNA synthesis. *Cell Death Differ* 2008, 15:1865–1874
- de Souza-Pinto NC, Harris CC, Bohr VA: p53 Functions in the incorporation step in DNA base excision repair in mouse liver mitochondria. *Oncogene* 2004, 23:6559–6568
- Achanta G, Sasaki R, Feng L, Carew JS, Lu W, Pelicano H, Keating MJ, Huang P: Novel role of p53 in maintaining mitochondrial genetic stability through interaction with DNA Pol gamma. *EMBO J* 2005, 24:3482–3492
- Bogenhagen DF, Rousseau D, Burke S: The layered structure of human mitochondrial DNA nucleoids. *J Biol Chem* 2008, 283:3665–3675
- Spelbrink JN: Functional organization of mammalian mitochondrial DNA in nucleoids: history, recent developments, and future challenges. *IUBMB Life* 2010, 62:19–32
- Park JY, Wang PY, Matsumoto T, Sung HJ, Ma W, Choi JW, Anderson SA, Leary SC, Balaban RS, Kang JG, Hwang PM: p53 Improves aerobic exercise capacity and augments skeletal muscle mitochondrial DNA content. *Circ Res* 2009, 105:705–712, 711 p following 712
- Matoba S, Kang JG, Patino WD, Wragg A, Boehm M, Gavrilova O, Hurley PJ, Bunz F, Hwang PM: p53 Regulates mitochondrial respiration. *Science* 2006, 312:1650–1653
- Schriner SE, Linford NJ, Martin GM, Treuting P, Ogburn CE, Emond M, Coskun PE, Ladiges W, Wolf N, Van Remmen H, Wallace DC, Rabinovitch PS: Extension of murine life span by overexpression of catalase targeted to mitochondria. *Science* 2005, 308:1909–1911
- Lewis W, Day BJ, Copeland WC: Mitochondrial toxicity of NRTI antiviral drugs: an integrated cellular perspective. *Nat Rev Drug Discov* 2003, 2:812–822
- Birkus G, Hitchcock MJ, Cihlar T: Assessment of mitochondrial toxicity in human cells treated with tenofovir: comparison with other nucleoside reverse transcriptase inhibitors. *Antimicrob Agents Chemother* 2002, 46:716–723
- Liang SH, Clarke MF: The nuclear import of p53 is determined by the presence of a basic domain and its relative position to the nuclear localization signal. *Oncogene* 1999, 18:2163–2166
- Liang SH, Clarke MF: Regulation of p53 localization. *Eur J Biochem* 2001, 268:2779–2783
- Mummenbrauer T, Janus F, Muller B, Wiesmuller L, Deppert W, Grosse F: p53 Protein exhibits 3'-to-5' exonuclease activity. *Cell* 1996, 85:1089–1099
- Shokolenko IN, Alexeyev MF, Robertson FM, LeDoux SP, Wilson GL: The expression of Exonuclease III from *E. coli* in mitochondria of breast cancer cells diminishes mitochondrial DNA repair capacity and cell survival after oxidative stress. *DNA Repair (Amst)* 2003, 2:471–482